

Self-supervised Pre-training for Semantic Segmentation in an Indoor Scene

Sulabh Shrestha¹, Yimeng Li¹ and Jana Košečka¹

Abstract—The ability to endow maps of indoor scenes with semantic information is an integral part of robotic agents which perform different tasks such as target driven navigation, object search or object rearrangement. The state-of-the-art methods use Deep Convolutional Neural Networks (DCNNs) for predicting semantic segmentation of an image as useful representation for these tasks. The accuracy of semantic segmentation depends on the availability and the amount of labeled data from the target environment or the ability to bridge the domain gap between test and training environment. We propose RegConsist, a method for self-supervised pre-training of a semantic segmentation model, exploiting the ability of the agent to move and register multiple views in the novel environment. Given the spatial and temporal consistency cues used for pixel level data association, we use a variant of contrastive learning to train a DCNN model for predicting semantic segmentation from RGB views in the target environment. The proposed method outperforms models pre-trained on ImageNet and achieves competitive performance when using models that are trained for exactly the same task but on a different dataset. We also perform various ablation studies to analyze and demonstrate the efficacy of our proposed method.

I. INTRODUCTION

Semantic segmentation has been used extensively for both semantic mapping [1] and also as input representation for training policies for embodied agents (e.g. policies for target driven or point goal navigation) that rely on visual perception [2], [3]. Training semantic segmentation model for a particular environment requires a large amount of per-pixel annotations [4] that is very costly and laborious. Alternatively for similar classes of environments that share a large subset of semantic labels, a model can be trained for the entire domain (say indoors environments) followed by domain adaptation [5]. In a robotic setting the agent is often able to move around and capture large amounts of visual data and the ability to estimate ego-motion and depth perception enables the agent to effectively associate multiple views of the same scene.

Recent years marked notable progress in various self-supervised methods for training large DCNN's from scratch without relying on commonly used backbones pre-trained on ImageNet. The existing techniques used various forms of contrastive learning and different pretext tasks such as predicting the masked portion of the image [7], predicting masks of objects [8] or predicting the rotation of the image [9]. The self-supervised pre-training is then followed by fine-tuning with a small fraction of the labeled data. Even though

¹Sulabh Shrestha, Yimeng Li and Jana Košečka are with the Department of Computer Science, George Mason University, 4400 University Dr, Fairfax, VA, USA {sshres2, yli44, kosecka}@gmu.edu

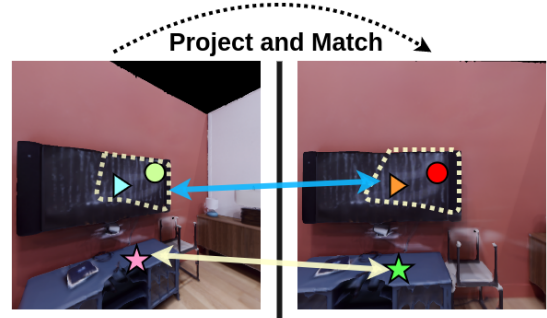


Fig. 1: Example of consistency. A pair of views from different location and pose of the agent inside an environment in Replica Dataset [6]. We find and match pixels across the view-pairs. In exact matching correspondence points are matched (yellow arrow). In region matching, any pixel across overlapping regions from the two views can be matched (blue arrow). Best viewed digitally or in color.

these models have been proven to be very effective, they are typically evaluated for image classification tasks.

In this paper we explore the use of self-supervision that comes from the spatial and temporal consistency between pairs of overlapping views and demonstrate how to pre-train Deep Convolutional Neural Network (DCNN) model for semantic segmentation using data captured in the environment of interest. We assume that within a single traversal path, the environment remains static so as to simplify the process of computing correspondences between neighboring views, that will be used for self-supervised training of the model.

Contribution 1) We propose RegConsist, a method for self-supervised pre-training of a semantic segmentation model using spatial and temporal consistency cues. We exploit correspondences between multiple views for generating positive examples for contrastive learning framework and evaluate the effect of different sampling strategies on the result. 2) We demonstrate that the resulting model can be fine-tuned with only a small fraction of image annotations, obtaining competitive or better performance in a novel indoor environment compared to fully supervised models. 3) We are the first to demonstrate that the Barlow twins loss [10] works well for semantic segmentation in an indoor environment. 4) We demonstrate the efficacy of our method on Replica [6] and AVD [11] datasets both qualitatively and quantitatively while using as low as 5 percent of the annotated data. 5) We perform extensive ablation studies to verify our method's performance including different starting conditions of the

segmentation model.

II. RELATED WORK

Our work relates to previous self-supervised learning efforts in robotics, exploiting the idea that robots are able to gather their own data and with proper training strategies do not have to rely on laborious labeling required for supervised training. In the past this idea was explored in the context of different tasks, such as pose-estimation [13], object detection [14], [15] and learning object specific visual representation for manipulation and tracking [16], to mention a few. Reinforcement learning and contrastive learning were the two most commonly used frameworks that spear-headed the technical advances in self-supervised learning in both computer vision and robotics. Below we review in more detail the works that are most relevant to our task of semantic segmentation.

A. Self-supervised Learning

To mitigate the need for large amounts of labeled data required for training deep models, self-supervised methods typically use various pretext tasks to generate training data. In the past, in single image setting, these included masked image modeling [7], object mask prediction [8], instance discrimination [17] and others. These auxiliary tasks provide the model with the desired objective to embed semantically similar inputs closer in the learned embedding space.

a) Contrastive Learning: Contrastive learning [18] has been a "workhorse" of self-supervised learning approaches for training DCNNs. It exploits the ability to associate (semantically) similar examples (positive pairs) and distinguish them from negative pairs as a supervision signal for learning suitable representations (embeddings). The existing approaches vary depending on the final task, CNN architectures (often using variations of Siamese Neural Network architectures), loss functions and methods for obtaining similar and dissimilar training examples. The most common concern in representation learning is to avoid model collapse. Authors in [17] consider each image as a separate class and the model is trained to disambiguate an image from other images in the dataset. MoCo [19] employed a dynamic memory bank [17] to store features from current the iteration of the model as negatives during training. In order to remove the requirement of memory bank, SimCLR [20] proposed to use negative pairs from the mini-batch itself but consequently necessitating a larger batch size. BYOL [21] further remove the need for the negative examples altogether, by introducing asymmetric architecture. Recently, [10] introduced a new objective function termed Barlow Twins, based on redundancy reduction, which removes the need for large batches and asymmetric models altogether.

b) Point Level Contrast.: While contrastive learning at the global image level has proven to be beneficial for image classification, the problems such as object detection and semantic segmentation where predictions are done at the object bounding box or pixel level, require disambiguation of

finer features. Getting pixel level positive pairs is more difficult than their image level counterpart. PixPro [22] follow SimSiam [23] like training but at the pixel level; the positives are obtained by thresholding the cosine distance between the features at the pixel level within a given image. Authors in [24] sample positive pixel pairs within regions obtained by k-means clustering of the initial features, while [25] circumvent the need of finding regions by dividing the image into a fixed $N \times N$ grid where each grid-cell is considered a separate region.

In situations where a small number of labeled examples is available one can approach learning using both cross entropy loss based on available labels along with self-supervised loss. This requires a momentum-updated teacher network along with a memory bank to associate features between examples outside of the images in a given iteration [26]. In order to obtain additional labels if labels are sparse [27], [28] proposed to use label propagation techniques. This however requires complete and accurate 3D reconstruction in order to fuse predictions from different frames.

Our work is most closely related to the efforts of self-supervised learning for object detection [15], [14] by using multiple views and view association to guide the training, but extends these ideas to dense pixel-level prediction tasks such as semantic segmentation.

III. METHOD

We assume a robotic agent with the ability to perceive and recover ego-motion and 3D structure of the environment and associate overlapping views of the same scene. This can be achieved with appropriate sensors such as a depth sensor or stereo camera or with the use of 3D structure and motion estimation techniques [29] or suitable SLAM approach [1]. To instantiate a self-supervised learning approach for semantic segmentation we propose a (**Region Consistency**) **RegConsist** method for temporal and spatial alignment of overlapping views that we describe next.

A. Temporal Consistency

Let I_1 and I_2 be two images captured by the agent in the fixed indoor environment. Assuming the availability of known intrinsic and extrinsic camera parameters and depth, we can associate the pixels in the overlapping views of the same scene using (1).

$$T_{1 \rightarrow 2}(I_1) = \{K(T_2^{-1}(T_1(K^{-1}(\mathbf{x}))) \quad \forall \mathbf{x} \in I_1\} \quad (1)$$

where, K is the intrinsic parameters of the camera, $T_1 = [R_1|t_1]$ is the camera pose for the image I_1 having rotation R_1 and translation t_1 with respect to a fixed coordinate system and \mathbf{x} is a pixel in I_1 . The operator $T_{1 \rightarrow 2}$ transforms the 2D pixel coordinates in I_1 to the 3D world coordinate system and projects it back to pixel coordinates in I_2 . We assume that reliable correspondences can be estimated either using learning based method [30] or, as in our case, with availability of the depth sensor. Let I_1^p and I_2^q be p^{th} and q^{th} pixels in the images I_1 and I_2 respectively. If the pixels belong to the same 3D location in the environment and

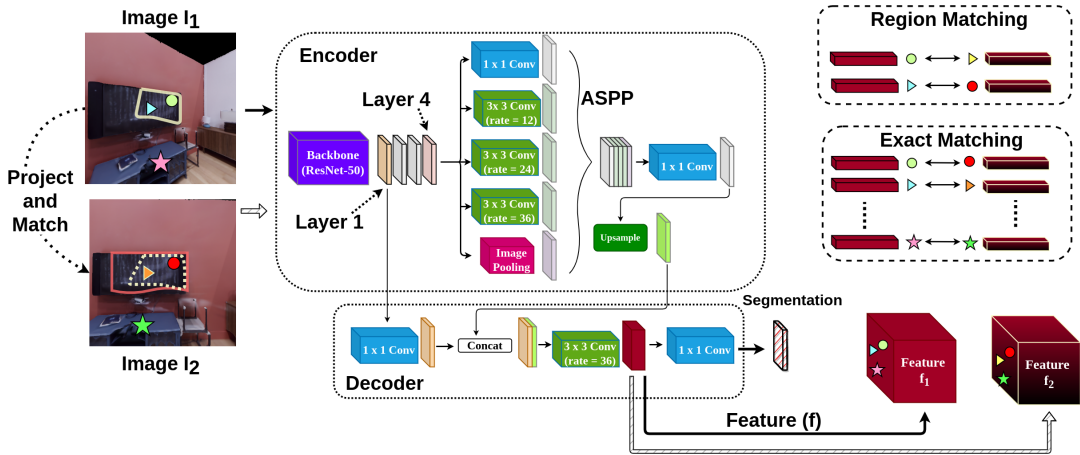


Fig. 2: Our proposed method. The segmentation model (DeepLabV3+ [12]) separately processes two views that capture the same part of the environment. Correspondence points are obtained from the two views. In exact matching only the correspondence points form positive pixels pairs. In region matching, regions are estimated for each view separately (yellow in I_1 and red in I_2). Then, points are matched from highly overlapping estimated regions across the views (in I_2 , red region with dotted yellow region projected from I_1). The positive pixel-pairs are aligned using Barlow Twins loss [10]. Best viewed digitally or in color.

unoccluded in both images, they are semantically identical. Let $S_t = \{(p, q) \mid p \in I_1, q \in I_2\}$ be the set of all such pixel-pairs. We consider all pairs in S_t as positives and enforce their features to be aligned across the views.

B. Spatial Consistency

The pixel-pairs we obtain from Section III-A may not have high variability, *i.e.* they might look very much similar across views, especially when views are close. Given the pixel p in I_1 and a small neighborhood region $\mathcal{N}(p)$ around the pixel, all pixels \hat{p} inside the region are highly likely to belong in the same class as p (yellow region in Figure 2). Similarly in I_2 , all $\hat{q} \in \mathcal{N}(q)$ belong to same class as q (dotted yellow region in I_2). Hence any pixel in $\mathcal{N}(p)$ can be matched with any pixel in $\mathcal{N}(q)$. Therefore, we also consider such pixel-pairs to be positives. Specifically, $S = \{(\hat{p}, \hat{q}) \mid p \in I_1, \hat{p} \in \mathcal{N}(p), q \in I_2, \hat{q} \in \mathcal{N}(q)\}$. It is important to note that $S_t \subset S$ because $p \in \mathcal{N}(p)$ and $q \in \mathcal{N}(q)$. Hence, the pairs are enforced to be aligned across overlapping and consistent regions (**Region Consistency**).

Regions can be estimated using unsupervised methods such as the efficient graph based segmentation method [31]. Because the regions are independently estimated across the views, they are not perfectly aligned. So to get highly overlapping regions, we need to find IoU between each region in I_1 with those in I_2 . This requires $O(|R_1| \cdot |R_2|)$ where $|R_1|$ and $|R_2|$ are the number regions in I_1 and I_2 . This is extremely slow to calculate in each iteration and hampers training speed. Therefore we devise a new algorithm to calculate this in $O(|R_1 \cap R_2|)$ where $|R_1 \cap R_2|$ is the number of overlapping regions between R_1 and R_2 that can be computed using the Cantor pairing function.

C. Pixel-Pair Sampling and Matching

While using all the pairs from the set S is possible, it is not an efficient method. So, we sample pixel-pairs from S in each batch. We proceed by first sampling the first pixel p from image I_1 . We then follow up by matching a suitable pixel q from image I_2 which is either spatially or temporally consistent as explained in Sections III-A and III-B.

In **random** sampling, we sample pixel p uniformly across the whole image I_1 . However, in indoor environments, class imbalance exists between large classes such as wall or floor and small classes such as cushion or plate as shown in Figure 3. To overcome this problem, in **balanced** sampling, we sample pixel p uniformly per region such that there are equal number of points from each region within a batch.

Once the first pixel p in the pair has been sampled from a view I_1 , we need to match it with a positive pixel from I_2 . In **exact** matching, we match the p with pixel q which is the exact correspondence of p that satisfies (1). To get variability between the pixels in the positive-pair, in **region** matching, we match p with q sampled uniformly from region R_2 that matches region R_1 in I_1 in which p resides, as explained in Section III-B.

D. Pair Loss

Let $|S|$ be the total number of pairs sampled in a batch. Let f_1^p and f_2^q be the features of pixels p and q obtained from images I_1 and I_2 respectively. For brevity, we overload the notation p and q to represent pixels as well as their features f_1^p and f_2^q respectively. In order to align the features of pixel-pairs, we use Barlow Twins loss [10] given by equation (2).

$$\mathcal{L}_{pair} = \sum_i (1 - C_{ii})^2 + \lambda \sum_i \sum_{j \neq i} C_{ij}^2 \quad (2)$$

where \mathcal{C} is the cross-correlation matrix computed between features p and q in the set S computed along the batch dimension and is given by equation (3).

$$c_{ij} = \frac{\sum_b p_i^{(b)} q_j^{(b)}}{\sqrt{\sum_b (p_i^{(b)})^2} \sqrt{\sum_b (q_j^{(b)})^2}} \quad (3)$$

where b indexes the batch of pixel-pairs and i and j index the vector dimensions of the features. The first term in the loss in (2) aligns the input feature-pairs while the second term minimizes the redundancy between each dimension of the features. More details can be found in [10].

While other contrastive losses can also be used, they require negative pairs or large batch-sizes or momentum encoders which we want to avoid for the sake of simplicity and efficiency. We also tried with SimSiam [23] like architectures and losses but initial experiments did not work.

E. Supervised Loss

When using labeled images for fine-tuning we use focal loss [32] to train the model only on the set of images that have labels. Using focal loss helps mitigate the problem of naturally present class imbalance in indoor environments.

IV. EXPERIMENTS

A. Dataset

We perform our experiments on Active Vision Dataset (AVD) [11] and Replica dataset [6]. AVD is a real-world dataset that consists of scenes from different apartments and offices. Each scene contains images taken by a robot in a grid-like manner and a few of the images are annotated. We use *Home_006_1* which contains 2412 images among which 43 images are annotated. Replica is a photo-realistic dataset that consists of multiple indoor environments. Both the datasets contain ground-truth depth as well as intrinsic and extrinsic parameters of the camera. Since AVD is a real-world dataset, it contains noisy and incomplete depth measurements. We start with Replica dataset to disambiguate the cause of errors between the noise in the data and our approach. Unless otherwise stated, we experiment on *frl_apartment_1* environment which has an apartment-like setting as shown in Figure 3. We use Habitat simulator [33] to move the agent in the environment and generate overlapping views similar to AVD.

We compare our model trained in self-supervised way with a segmentation model already trained on ADE20K dataset [4], [34]. The class labels from Replica and AVD are both separately mapped to those in ADE20K dataset resulting in 52 and 66 classes respectively. We discard classes that do not have an unambiguous overlap.

View-Pair Selection We heuristically sample informative pairs of images, by considering uniformly sampled views on a grid and selecting neighboring views with varying degree of overlap as characterized by Intersection over Union (IoU) measure. The view pairs with IoU in the range of $[iou_l, iou_h]$ are selected for training. This sampling process

reduces computation during training as it needs only be done once per environment for all the experiments.

B. Implementation Details

We use a slightly modified version of DeeplabV3+ [12] as our segmentation model as shown in Figure 2 with ResNet50 [35] backbone. We randomly initialize all the weights of the model.

a) Pre-training: We pre-train the models using all view-pairs sampled as explained in IV-A using $iou_l = 0.3$ and $iou_r = 0.9$. To generate regions, we use the efficient graph based segmentation method [31] with $scale = 250$ and $sigma = 2000$. We obtained these parameters by calculating IoU with available 5% ground truth annotation in Replica for various values. We take the output before the final layer as the feature on which the pair-loss is calculated as explained in Section III-D. We resize the feature map to original input resolution using nearest neighbor interpolation to project and match across views. We use a batch-size of 16 i.e. 32 pairs of related views by default. In each batch, we sample $|S| = 81920$ pixels. We use strong and weak image augmentations for I_1 and I_2 respectively, which we found performs better than using strong augmentations for both. With Barlow Twins loss we also found that it helpful to use a norm gradient clipping of 5 and $\lambda = 0.005$ [10]. We use a learning rate of 0.01 for 50K iterations with a cosine decay scheduler [36] which decreases the learning rate by a factor of 10. We use a learning rate warm-up period of 2500 iterations. We use a V100 GPU to train the models.

b) Fine-tuning: For fine-tuning we use ground truth annotation from 5% (16) of all the images in the Replica environment and remaining image annotations for testing. For AVD, we create 2 sub-datasets. In *AVD-easy*, we choose 5 annotated images for testing that have high overlap with the training set which consists of 38 (1.57%) of the 2412 images. However, in *AVD-hard*, we fine-tune on 24 (1%) images randomly chosen while testing on the remaining 19. For fair analysis, we use the same set of images for training and testing across all the experiments. We use a learning rate of 0.01 with a polynomial scheduler for 80K iterations and a weight decay of $5e^{-4}$. For the segmentation model trained on ADE20K, we found that using a learning rate of 0.001 is better than 0.01 because the model is already suitable for segmentation out-of-the-box.

C. Baselines

First, we try our approach using exact pixel matching. Specifically, we project points from one image/view of the environment to another as mentioned in section III-A and train using the full set of corresponding pixel-pairs. While looking at the predictions made by our model, we found that most of the wrongly predicted pixels were assigned to background classes wall or floor.

Hypotheses: We hypothesize two possible reasons for the poor performance in exact matching. The first reason is the inherent class imbalance in indoor environments. The second reason is that the pixel-pairs between the two views have low

TABLE I: Supervised Baselines

Name	Supervision	Sampling	Matching	mIoU
BaR	labels	Balanced	Region	73.4
BaX	labels	Balanced	eXact	61.2
RaR	labels	Random	Region	48.6
RaX	labels	Random	eXact	60.5

TABLE II: Results on Replica

Weights	Model-weights	Dataset	Pre-Training	mIoU
Random	–	–	–	43.9
ImageNet	ResNet50	ImageNet	classification	48.7
ADE20K	DeepLabV3+	ADE20K	segmentation	<u>59.2</u>
PixPro1x [22]	ResNet50	ImageNet	self-sup	53.7
PixPro4x [22]	ResNet50	ImageNet	self-sup	54.7
RegConsist	DeepLabV3+	Replica	self-sup	62.7

variability between them i.e. the pixels look similar across the views. In order to verify this hypothesis, we perform experiments by assuming the availability of ground truth labels while pre-training. This gives us an upper bound of our proposed method. We try all combinations of sampling and matching techniques for the pixel-pairs as explained in Section III-C but using ground truth labels as regions.

The results for the baseline experiments are shown in Table I. Because of the class imbalance, random sampling (RaX, RaR) results in a higher number of samples from large classes which overweight the smaller classes. Balanced sampling (BaX, BaR) is better with either of the matching methods because an equal number of pairs are sampled from each class. This confirms our class-imbalance hypothesis. Region matching (BaR) is better than exact matching (BaX) with balanced sampling. This shows that it is also important to match non-corresponding pixels from the same class. Hence, this validates our low variability hypothesis. We also point out that sampling in a class-balanced way is more important than matching because in balanced sampling method, both matching strategies are higher than those in random sampling. Interestingly, when performing random sampling we observe that it is best to match exact projection (RaX). However, matching this way limits the possible number of pairs that can be formed so many possible informative pairs can be missed. This is verified with our best performing model that uses region matching.

D. Results

We use estimated regions during training and apply our RegConsist approach on Replica dataset. The results are shown in Table II. To compare, we change the initialization

TABLE III: Results on AVD

Weights	mIoU (AVD-easy)	mIoU (AVD-hard)
Random	66.7	49.1
ADE20K	69.3	69.1
RegConsist (Ours)	69.5	64.8

TABLE IV: Number of Labeled Examples

Labeled Images	5%	10%	20%	30%
ADE20K	59.2	67.2	76.8	80.1
RegConsist (Ours)	62.7	67.8	77.3	80.5

of DeepLabV3+ with other trained or pre-trained models. ImageNet is the ResNet50 model trained in a supervised manner for image classification on the ImageNet dataset [37]. Similarly ADE20K model was trained on ADE20K dataset [4], [34] for semantic segmentation in a supervised manner for 200 epochs which reaches an mIoU of 39.8 in the ADE20K validation set. PixPro1x and PixPro4x [22] were both trained on ImageNet in a self-supervised manner using single view augmentation techniques on the ImageNet dataset for 100 and 400 epochs respectively. Our method performs better than even the DeepLabV3+ model trained for ADE20K dataset which shows that it is important to pre-train the model in a new environment. It still does not reach the ground truth baseline because the estimated regions do not precisely match the ground truth labels.

Similarly, we compare our method with the worst and the best model from Replica, excluding ours, on AVD sub-datasets. The results are shown in Table III. AVD-easy is easy even for the Random initialization but AVD-hard is very difficult. RegConsist does not perform better than ADE20K on AVD-hard. We suspect that the gap between AVD and ADE20K is simpler (both are real world with indoor images) so ADE20K is able to utilize its existing knowledge. However the large domain gap makes it difficult to do the same in Replica. This demonstrates that our method is very good in situations where the domain gap is large or when there is no dataset on which supervised learning can be done beforehand. Similarly, our method depends on the precision of the regions we obtain and we did not tune the regions for AVD unlike Replica.

E. Ablations

Number of Labeled examples We experiment by changing the amount of labeled images for fine-tuning. We train for 80K iterations instead of 20K. The results are shown in table IV. As can be seen, our method performs better than that trained on ADE20K in every case. The gap between the performance decreases the more labeled examples are available. This shows that our model is more suited in the fewer annotation regime.

Starting weights Instead of starting from scratch during pre-training, we experiment with other weight initialization as shown in Table V. Changing the start weights does not affect the performance much because our method is inherently instance specific. Region consistency is limited to matching spatially and visually similar pixels in the images; an object may be covered by one of the regions but two objects from the same class will not have a direct association between them. Hence, any category-specific information obtained from weight initialization is unused and/or lost. So

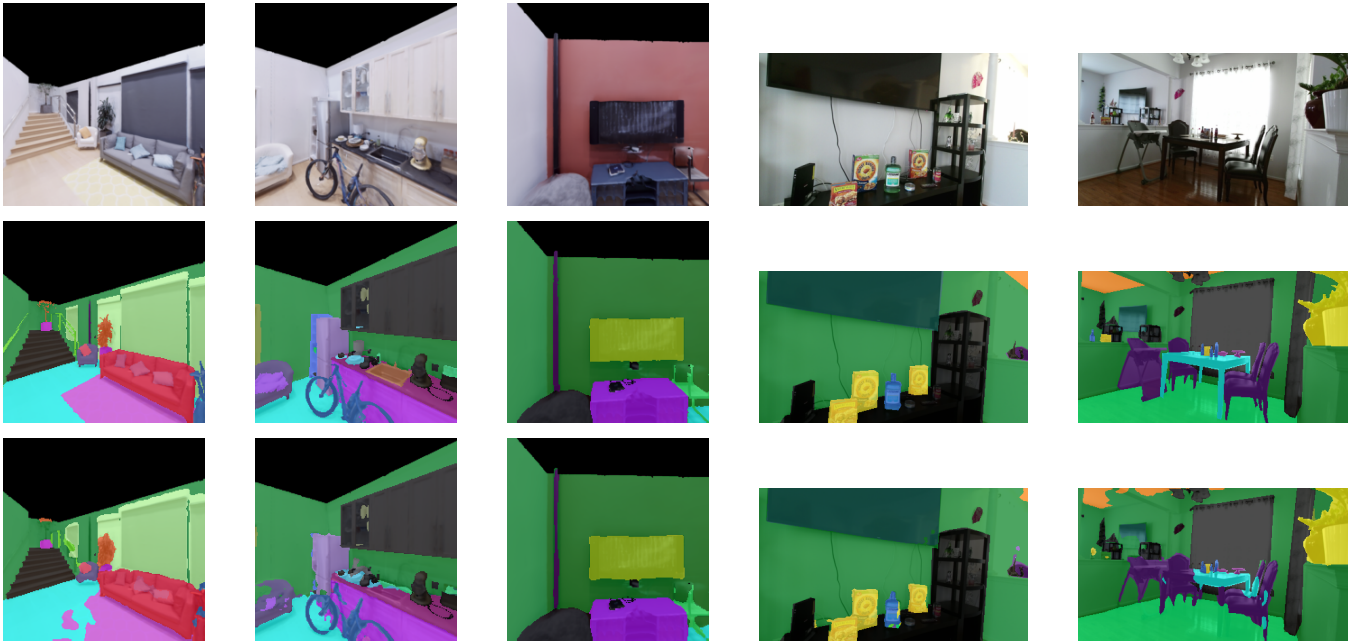


Fig. 3: RGB images (top row), ground truth (middle row) and predictions from RegiCon (bottom row). Images from the Replica dataset [6] (3 leftmost columns) and AVD dataset [11] (2 rightmost columns). Dark pixels in segmentation images do not have a valid class.

TABLE V: Starting Weights

Initialization	Dataset	Training	mIoU
Random	–	None	57.0
ImageNet-sup	ImageNet	Supervised	56.7
PixPro-400 [22]	ImageNet	Self-supervised	57.4

the model learns in a bottom-up approach: in the pre-training phase instances are learned followed by categories in the fine-tuning phase.

Image IoU threshold When choosing view-pairs from the environment, we check various IoU threshold ranges by changing the values of iou_l and iou_h and fine-tuning for 20K iterations. From Figure 4, we can see that threshold [7-9] produces the worst result of 54.4 because the images in the pairs are very similar to each other, obtained through minor movements of the agent. We find that threshold [3-7] produces the best results which shows that it is important to keep a balance between similar and dissimilar view-pairs.

V. CONCLUSION

We have demonstrated the effectiveness of self-supervised pre-training of semantic segmentation models in an indoors environment by exploiting spatial and temporal consistency between regions in overlapping views. The method exploits the ability to register neighboring views of indoors scenes and uses efficient generation of positive training examples for contrastive learning framework. The proposed approach was validated through several experiments and ablation studies, demonstrating the effects of different choices of sampling

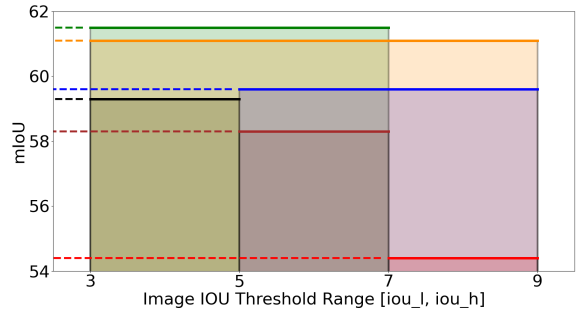


Fig. 4: Image IoU threshold range vs accuracy.

strategies, amounts of labeled data as well as comparisons with alternative baseline approaches that rely on fine-tuning of models pre-trained on labeled data. We also investigate properties of our approach by starting from various weight initialization led us to discover that it gains instance specific knowledge. We argue and show that this level of information helps the model to better learn category specific information in the fine-tuning stage. We show that our approach, Reg-Consist, allows the agent to learn as good as a model trained on labeled data from a related domain. The assumption of availability of labeled images from a similar domain is not valid for all possible domains. Our approach is especially beneficial in such scenarios.

REFERENCES

- [1] C. Cadena, L. Carlone, H. Carrillo, Y. Latif, D. Scaramuzza, J. Neira, I. Reid, and J. J. Leonard, “Past, present, and future of simultaneous

- localization and mapping: Toward the robust-perception age,” *IEEE Transactions on Robotics*, vol. 32, no. 6, 2016.
- [2] D. S. Chaplot, D. P. Gandhi, A. Gupta, and R. R. Salakhutdinov, “Object goal navigation using goal-oriented semantic exploration,” in *Advances in Neural Information Processing Systems*, H. Larochelle, M. Ranzato, R. Hadsell, M. Balcan, and H. Lin, Eds., vol. 33. Curran Associates, Inc., 2020, pp. 4247–4258.
 - [3] G. Georgakis, B. Bucher, K. Schmeckpeper, S. Singh, and K. Daniilidis, “Learning to map for active semantic goal navigation,” in *International Conference on Learning Representations*, 2022. [Online]. Available: <https://openreview.net/forum?id=swrMQtr6wN>
 - [4] B. Zhou, H. Zhao, X. Puig, S. Fidler, A. Barriuso, and A. Torralba, “Scene parsing through ade20k dataset,” in *Proceedings of the IEEE Conference on Computer Vision and Pattern Recognition*, 2017.
 - [5] J. Hoffman, E. Tzeng, T. Park, J.-Y. Zhu, P. Isola, K. Saenko, A. Efros, and T. Darrell, “CyCADA: Cycle-consistent adversarial domain adaptation,” in *Proceedings of the 35th International Conference on Machine Learning*, ser. Proceedings of Machine Learning Research, J. Dy and A. Krause, Eds., vol. 80. PMLR, 10–15 Jul 2018, pp. 1989–1998. [Online]. Available: <https://proceedings.mlr.press/v80/hoffman18a.html>
 - [6] J. Straub, T. Whelan, L. Ma, Y. Chen, E. Wijmans, S. Green, J. J. Engel, R. Mur-Artal, C. Ren, S. Verma, A. Clarkson, M. Yan, B. Budge, Y. Yan, X. Pan, J. Yon, Y. Zou, K. Leon, N. Carter, J. Briales, T. Gillingham, E. Mueggler, L. Pesqueira, M. Savva, D. Batra, H. M. Strasdat, R. D. Nardi, M. Goesele, S. Lovegrove, and R. Newcombe, “The Replica dataset: A digital replica of indoor spaces,” *arXiv preprint arXiv:1906.05797*, 2019.
 - [7] K. He, X. Chen, S. Xie, Y. Li, P. Dollár, and R. Girshick, “Masked autoencoders are scalable vision learners,” in *Proceedings of the IEEE/CVF Conference on Computer Vision and Pattern Recognition (CVPR)*, June 2022, pp. 16000–16009.
 - [8] O. J. Hénaff, S. Koppula, E. Shelhamer, D. Zoran, A. Jaegle, A. Zisserman, J. Carreira, and R. Arandjelović, “Object discovery and representation networks,” *arXiv preprint arXiv:2203.08777*, 2022.
 - [9] S. Gidaris, P. Singh, and N. Komodakis, “Unsupervised representation learning by predicting image rotations,” in *International Conference on Learning Representations*, 2018. [Online]. Available: <https://openreview.net/forum?id=S1v4N2i0>
 - [10] J. Zbontar, L. Jing, I. Misra, Y. LeCun, and S. Deny, “Barlow twins: Self-supervised learning via redundancy reduction,” in *Proceedings of the 38th International Conference on Machine Learning*, ser. Proceedings of Machine Learning Research, M. Meila and T. Zhang, Eds., vol. 139. PMLR, 18–24 Jul 2021, pp. 12310–12320. [Online]. Available: <https://proceedings.mlr.press/v139/zbontar21a.html>
 - [11] P. Ammirato, P. Poirson, E. Park, J. Kosecka, and A. C. Berg, “A dataset for developing and benchmarking active vision,” in *IEEE International Conference on Robotics and Automation (ICRA)*, 2017.
 - [12] L.-C. Chen, Y. Zhu, G. Papandreou, F. Schroff, and H. Adam, “Encoder-decoder with atrous separable convolution for semantic image segmentation,” in *Proceedings of the European Conference on Computer Vision (ECCV)*, September 2018.
 - [13] X. Deng, Y. Xiang, A. Mousavian, C. Eppner, T. Bretl, and D. Fox, “Self-supervised 6d object pose estimation for robot manipulation,” in *IEEE ICRA*, 2021.
 - [14] E. Pot, A. Toshev, and J. Kosecka, “Self-supervised object discovery and detection,” *preprint arXiv*, 2018.
 - [15] Z. Fang, A. Jain, G. Sarch, A. W. Harley, and K. Fragkiadaki, “Move to see better: Self-improving embodied object detection,” in *BMVC*, 2021.
 - [16] L. Manuelli, Y. Li, P. Florence, and R. Tedrake, “Keypoints into the future: self-supervised correspondence in model-based reinforcement learning,” in *Conference on Robot Learning*, 2020.
 - [17] Z. Wu, Y. Xiong, S. X. Yu, and D. Lin, “Unsupervised feature learning via non-parametric instance discrimination,” in *Proceedings of the IEEE Conference on Computer Vision and Pattern Recognition (CVPR)*, June 2018.
 - [18] R. Hadsell, S. Chopra, and Y. LeCun, “Dimensionality reduction by learning an invariant mapping,” in *2006 IEEE Computer Society Conference on Computer Vision and Pattern Recognition (CVPR’06)*, vol. 2, 2006, pp. 1735–1742.
 - [19] K. He, H. Fan, Y. Wu, S. Xie, and R. Girshick, “Momentum contrast for unsupervised visual representation learning,” in *Proceedings of the IEEE/CVF Conference on Computer Vision and Pattern Recognition (CVPR)*, June 2020.
 - [20] T. Chen, S. Kornblith, M. Norouzi, and G. Hinton, “A simple framework for contrastive learning of visual representations,” in *Proceedings of the 37th International Conference on Machine Learning*, ser. Proceedings of Machine Learning Research, H. D. III and A. Singh, Eds., vol. 119. PMLR, 13–18 Jul 2020, pp. 1597–1607. [Online]. Available: <https://proceedings.mlr.press/v119/chen20j.html>
 - [21] J.-B. Grill, F. Strub, F. Altché, C. Tallec, P. Richemond, E. Buchatskaya, C. Doersch, B. Avila Pires, Z. Guo, M. Gheshlaghi Azar, B. Piot, k. kavukcuoglu, R. Munos, and M. Valko, “Bootstrap your own latent - a new approach to self-supervised learning,” in *Advances in Neural Information Processing Systems*, H. Larochelle, M. Ranzato, R. Hadsell, M. Balcan, and H. Lin, Eds., vol. 33. Curran Associates, Inc., 2020, pp. 21271–21284.
 - [22] Z. Xie, Y. Lin, Z. Zhang, Y. Cao, S. Lin, and H. Hu, “Propagate yourself: Exploring pixel-level consistency for unsupervised visual representation learning,” in *Proceedings of the IEEE/CVF Conference on Computer Vision and Pattern Recognition (CVPR)*, June 2021, pp. 16684–16693.
 - [23] X. Chen and K. He, “Exploring simple siamese representation learning,” in *Proceedings of the IEEE/CVF Conference on Computer Vision and Pattern Recognition (CVPR)*, June 2021, pp. 15750–15758.
 - [24] F. ZHANG, P. Torr, R. Ranftl, and S. Richter, “Looking beyond single images for contrastive semantic segmentation learning,” in *Advances in Neural Information Processing Systems*, M. Ranzato, A. Beygelzimer, Y. Dauphin, P. Liang, and J. W. Vaughan, Eds., vol. 34. Curran Associates, Inc., 2021, pp. 3285–3297.
 - [25] Y. Bai, X. Chen, A. Kirillov, A. Yuille, and A. C. Berg, “Point-level region contrast for object detection pre-training,” in *Proceedings of the IEEE/CVF Conference on Computer Vision and Pattern Recognition (CVPR)*, June 2022, pp. 16061–16070.
 - [26] I. Alonso, A. Sabater, D. Ferstl, L. Montesano, and A. C. Murillo, “Semi-supervised semantic segmentation with pixel-level contrastive learning from a class-wise memory bank,” in *Proceedings of the IEEE/CVF International Conference on Computer Vision (ICCV)*, October 2021, pp. 8219–8228.
 - [27] J. McCormac, A. Handa, A. Davison, and S. Leutenegger, “Semanticfusion: Dense 3d semantic mapping with convolutional neural networks,” in *2017 IEEE International Conference on Robotics and Automation (ICRA)*, 2017, pp. 4628–4635.
 - [28] R. A. Rosu, J. Quenzel, and S. Behnke, “Semi-supervised Semantic Mapping Through Label Propagation with Semantic Texture Meshes,” *International Journal of Computer Vision*, vol. 128, no. 5, pp. 1220–1238, May 2020. [Online]. Available: <http://link.springer.com/10.1007/s11263-019-01187-z>
 - [29] Y. Ma, S. Soatto, J. Kosecka, and S. S. Sastry, *An Invitation to 3-D Vision: From Images to Geometric Models*. SpringerVerlag, 2003.
 - [30] P. Truong, M. Danelljan, F. Yu, and L. Van Gool, “Warp consistency for unsupervised learning of dense correspondences,” in *Proceedings of the IEEE/CVF International Conference on Computer Vision (ICCV)*, October 2021, pp. 10346–10356.
 - [31] P. F. Felzenszwalb and D. P. Huttenlocher, “Efficient graph-based image segmentation,” *International Journal of Computer Vision*, vol. 59, pp. 167–181, 2004.
 - [32] T.-Y. Lin, P. Goyal, R. Girshick, K. He, and P. Dollár, “Focal loss for dense object detection,” in *Proceedings of the IEEE International Conference on Computer Vision (ICCV)*, Oct 2017.
 - [33] M. Savva, A. Kadian, O. Maksymets, Y. Zhao, E. Wijmans, B. Jain, J. Straub, J. Liu, V. Koltun, J. Malik, D. Parikh, and D. Batra, “Habitat: A platform for embodied ai research,” in *Proceedings of the IEEE/CVF International Conference on Computer Vision (ICCV)*, October 2019.
 - [34] B. Zhou, H. Zhao, X. Puig, T. Xiao, S. Fidler, A. Barriuso, and A. Torralba, “Semantic understanding of scenes through the ade20k dataset,” *International Journal of Computer Vision*, vol. 127, no. 3, pp. 302–321, 2019.
 - [35] K. He, X. Zhang, S. Ren, and J. Sun, “Deep residual learning for image recognition,” in *2016 IEEE Conference on Computer Vision and Pattern Recognition (CVPR)*, 2016, pp. 770–778.
 - [36] I. Loshchilov and F. Hutter, “SGDR: Stochastic gradient descent with warm restarts,” in *International Conference on Learning Representations*, 2017. [Online]. Available: <https://openreview.net/forum?id=Skq89Sccx>
 - [37] J. Deng, W. Dong, R. Socher, L.-J. Li, K. Li, and L. Fei-Fei, “Imagenet: A large-scale hierarchical image database,” in *2009 IEEE Conference on Computer Vision and Pattern Recognition*, 2009, pp. 248–255.